Journal of Building Engineering 28 (2020) 101065

Contents lists available at ScienceDirect

Journal of Building Engineering

journal homepage: http://www.elsevier.com/locate/jobe

Reliability assessment of truss structures with natural frequency constraints using metaheuristic algorithms

Seyed Rohollah Hoseini Vaez *, Hashem Mehanpour, Mohammad Ali Fathali

Department of Civil Engineering, Faculty of Engineering, University of Qom, Qom, Iran

ARTICLE INFO

Keywords:
Reliability index
Truss structures
Frequency constraints
Failure probability
Metaheuristic algorithms
Optimization

ABSTRACT

The failure probability (reliability index) and evaluation of safety of structures is a subject of interest in structural engineering. In order to calculate the reliability index, moment methods require an explicit mathematical form of the limit state function and gradient of this function, and simulation methods are dependent on a large number of evaluations of this function. In this study, in order to reduce computational efforts, the optimization problem is formulated so it can calculate the reliability index for structural problems with an implicit limit-state function. For this purpose, the objective function is formulated based on the Hasofer and Lind method, and the limit state function is defined based the first mode frequency. The random variables consist of modulus of elasticity, material density, non-structural mass, and cross-sectional area. To evaluate accuracy of the proposed approach in estimating the reliability index, four truss structures are selected and their reliability index is calculated by using six meta-heuristic algorithms including WEO, AWEO, CBO, ECBO, VPS, and EVPS. Compared with the Monte Carlo simulation method, the proposed approach shows acceptable performance.

1. Introduction

The analysis and design of structures based on reliability theory is a topic that has recently been seriously considered. This attention is associated with the random nature of the structural parameters, such as material properties, external loads, geometric characteristics of the cross section of members, geometric dimensions of structures, and so on. Using reliability theory in structural systems, the uncertainties caused by the statistical nature of the structural parameters can be introduced as mathematical equations, while the safety and performance considerations are applied quantitatively in the design process [1,2]. Assessment of the probability of failure or calculation of reliability index is a fundamental issue in the reliability analysis of structures. One of the simplest and most basic first-order estimation methods for the calculation of reliability index was proposed by Cornell in 1969 [3]. In 1974, Hasofer and Lind defined the new reliability index as the minimum geometric distance between the origin and the reduced limit state function [4]. In the past decades, researchers have provided many different methods to calculate the probability of failure or reliability index that can be categorized as follows:

Moment methods: These methods are based on various moments of the random variables such as mean value, variance, and other higher order moments. Using gradient methods, the shortest distance of the limit state function is defined from the center of the standard normal coordinate system, called the reliability index. Then, the probability of failure is achieved by having this index [5–8].

Simulation methods: In these methods, like the Monte Carlo simulation, random samples are generated based on the sampling probability density function for random variables. Then the limit state function is calculated for each sample. The probability of failure is obtained by dividing the number of times that the limit state function has become negative by the total number of simulations [9–13]. Since the Monte Carlo simulation method requires a large number of simulations and results in a high volume evaluations of limit state function, researchers are moving towards new efficient simulation methods such as: Asymptotic Sampling (AS) [14], Weighted Simulation (WS) [15], Asymptotic Weighted Simulation (AWS) [16].

Meta-heuristic methods: These methods transform the reliability index calculation problem into a constrained optimization problem. In these methods, the shortest distance of the limit state function from the origin of the standard normal coordinate system is considered as the objective function and constraints is also introduced as the limit state function. Population-based meta-heuristic methods are used to find the reliability index [17–23]. These methods have the following advantages:

* Corresponding author.
E-mail address: hoseinivaez@qom.ac.ir (S.R. Hoseini Vaez).

https://doi.org/10.1016/j.jobe.2019.101065
Received 11 May 2019; Received in revised form 7 November 2019; Accepted 9 November 2019
Available online 11 November 2019

- Despite moment methods, there is no need to the explicit mathematical form of limit state function and the calculations can be performed with merely having access to the implicit form.
- In moment methods, it is necessary to calculate first-order (such as FORM method) and second-order (such as SORM method) derivatives for the limit state function. However, this method does not require derivatives of the limit state function.
- FORM and SORM methods, respectively, consider the limit state function with first-order and second-order approximations, which would have errors themselves; therefore, none of the FORM and SORM methods is a powerful method for complex limit state functions such as nonlinear limit state functions, functions having several points of failure, or a combination of limit state functions.
- Simulation methods require a large number of simulations (especially for low probability of failure), and as a result, a high volume of evaluation of limit state function. Moreover, the point with the most probability of failure, i.e. the point with the smallest distance from the origin in the standard normal space, which leads to a zero limit state function, is not calculated in simulation methods, while it is calculated in meta-heuristic methods.
- Despite the simplicity of moment methods, the answer to the problem is highly dependent on the starting point of the search, and in problems with multiple design points, it may converge to the optimal local response, which is not desirable. However, meta-heuristic methods are capable of leaving the local optimum and can be independent of the initial values of the search points.

Previous researchers have applied meta-heuristic algorithms to calculate the reliability index of mathematical problems, but fewer studies have been performed on structural problems whose limit state functions are not available in the form of explicit mathematical formulas.

Therefore, in this paper, population-based meta-heuristic algorithms are used to calculate the reliability index of the structures. These algorithms include WEO, AWEO, CBO, ECBO, VPS and EVPS which is used for various optimization problem [24–27]. In this paper, four truss structures are expressed with frequency probabilistic constraints. Each problem is presented with 6 meta-heuristic algorithms for each of which 100 runs are performed and finally, the results are compared with each other.

The rest of this article is organized as follows: Part 2 provides a brief overview of the concept of reliability assessment. In Part 3, optimization algorithms are briefly presented. Four numerical problems of truss structures with 10, 72, 52, and 120 members are presented in Part 4. All of them are set to frequency constraint and finally, Part 5 is devoted to the conclusion of the study.

2. Reliability assessment

Assessment of Probability of Failure (P_f) is a fundamental issue in reliability analysis of structures. In this section, different classical methods of this theory are expressed. In these methods, probabilistic uncertainties are considered as random variables in the design model. The performance of each structure can be expressed by the function of the basic random variables of the structure, called the Limit State Function (LSF), so that the positive value of the limit state function denotes the safety and the negative value of the state limit function indicates the failure. In analysis of a system, the failure area is defined by the function $g(R, Q) = [(R\text{-}Q \leq 0)]$ in which R and Q represent the values of resistance and the load effects on the structure, respectively. The probability of structural failure can be expressed by considering the joint probability density function, $f_{R,Q}$, for the random variables of R and Q as follows:

$$P_f = P\{g(R,Q) \leq 0\} = \int_{g \leq 0} f_{R,Q}\, dR\, dQ \tag{1}$$

Obtaining a direct answer to this integral is difficult due to the complexity of the joint probability density function (especially for variables with non-normal distribution), and in most cases, it is done using simplifying assumptions. These assumptions are presented in two approximation and simulation methods. Approximation methods based on the reliability index use the first and second-order Taylor expansion of limit state function. Simulation-based methods calculate the probability of failure directly and using sampling.

One of the simplest and most basic first-order estimation methods for reliability is provided by Cornell [3] in 1967. This method is based on the separation of the health area ($g > 0$) and the failure area ($g \leq 0$), and the linear expansion of the limit state function around the mean point. Finally, the definition of the reliability index, β, is expressed as follows:

$$\beta = \frac{E[g]}{\sqrt{Var[g]}} = \frac{E[R] - E[Q]}{\sqrt{Var[R] - Var[Q]}} \quad \text{or} \quad \beta = \frac{\mu_g}{\sigma_g} = \frac{\mu_R - \mu_Q}{\sqrt{\sigma_R^2 - \sigma_Q^2}} \tag{2}$$

where g indicates the limit state function and is calculated according to Eq. (3).

$$g = g(R,Q) = R - Q \tag{3}$$

In this equation, $E[g] = \mu_g$, $Var[g] = \sigma_g^2$, and σ_g indicate the mean value, variance, and standard deviation of g function.

Cornell method is not very efficient in solving reliability problems due to non-consideration of the probability distribution function of random variables, and also because of obtaining different answers when the expression of limit state function is changed.

In 1974, Hasofer and Lind [4] provided a new reliability index based on Cornell's idea and using the linear form of the limit state function in combination with a map to transfer random variables from the design space to the standard normal space (with mean zero and standard deviation of unit). This index is defined as the minimum geometric distance between the origin and the reduced limit state function. According to the definition given by Hasofer and Lind, the design point is a point on the limit state function ($g = 0$) that has the least distance from the origin in the standard normal space; this point is also known as the point with the most probable failure (Most Probable Point-MPP). The distance from this point to the origin is considered as a reliability index, which enables estimation of the probability of structural failure by the equation $P_f = \Phi(\text{-}\beta)$ where Φ is the standard normal cumulative distribution function. Therefore, an optimization problem needs to be applied according to Eq. (4) in order to calculate the design point.

$$\begin{aligned} &\textit{Find} && U = \{u_1, u_2, u_3, \ldots, u_n\} \\ &\textit{Min} && \beta = \sqrt{\sum_{i=1}^{n} {u_i}^2} = \sqrt{u^t u} = \sqrt{u_1^2 + u_2^2 + u_3^2 + \ldots\ldots + u_n^2} \\ &\textit{Subject to} && g(U) = 0 \end{aligned} \tag{4}$$

In this equation, u_i indicates the value of the ith random variable in the standard normal space and n represents the number of random variables. This parameter is calculated for random variables with normal distribution through the following equation:

$$u_i = \frac{x_i - \mu_{x_i}}{\sigma_{x_i}} \tag{5}$$

In which μ_{x_i} and σ_{x_i} are the mean and standard deviation of x_i random variable, respectively.

The idea presented by Hadofer and Lind is not applied in the case of random variables with non-normal distribution. In 1976, Rackwitz and Fiessler resolved this limitation by using an equivalent two-parameter normal transfer method [28]. The most commonly used method to transfer the state of a non-normal variable into an equivalent standard normal variable is indicated by Eq. (6).

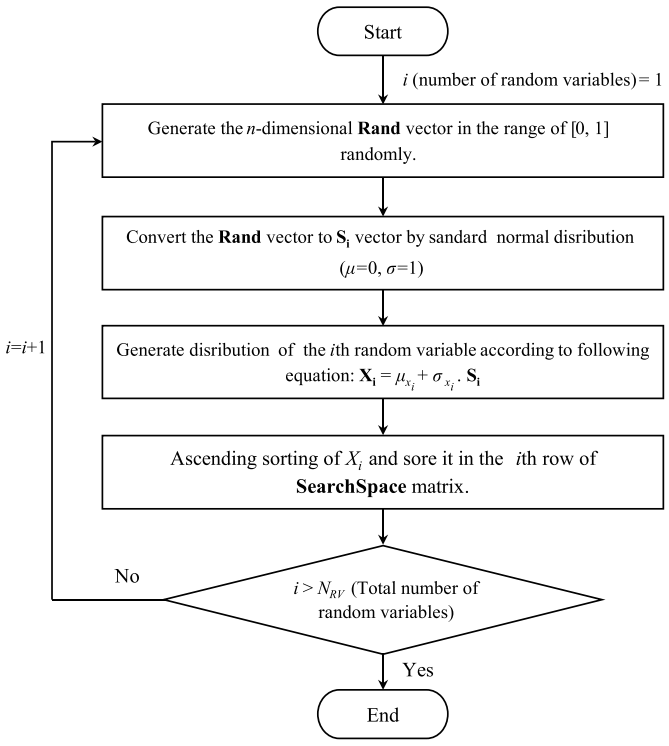

Fig. 1. Flowchart of generating the search space.

$$\sigma_x^e = \frac{1}{f_x(x^*)}\phi\left[\Phi^{-1}(F_x(x^*))\right]$$
$$\mu_x^e = x^* - \sigma_x^e\left[\Phi^{-1}(F_x(x^*))\right] \quad (6)$$
$$U = \frac{x^* - \mu_x^e}{\sigma_x^e}$$

In this equation, μ_x^e, σ_x^e, f_x, and F_x indicate equivalent normal mean, equivalent normal standard deviation, probability density function (PDF), and cumulative distribution function (CDF) of x^* variable, respectively, while parameters ϕ and Φ represent PDF for the standard normal distribution and CDF for the standard normal distribution, respectively. If a variable has a non-normal probability distribution function, the above method transfers the variable into a standard normal space using the map; this causes a significant increase in the degree of non-linearity of the limit state function and subsequently reduces the accuracy of the calculation.

In this paper, in order to apply the type of variables distribution, the search space of the optimization problem for n samples of each variable is created according to Fig. 1. Optimization algorithm for the search of optimal solution generates a vector whose dimension is the total number of random variables (N_{RV}) of integers in the interval [1, n]. According to the values of this vector and Eq. (5), the vector U in Eq. (4) is generated from the search space of the problem (**SearchSpace** matrix). To

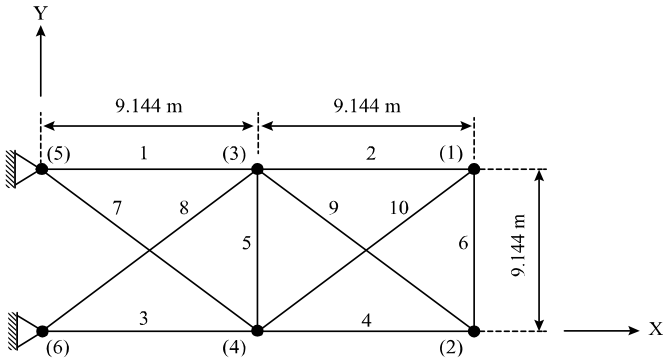

Fig. 3. Schematic of the planar 10-bar truss.

Table 1
Random variables for the 10-bar truss problem.

Random Variable, unit	Mean	COV
E (Modulus of elasticity), N/m^2	6.98×10^{10}	5%
ρ (Material density), kg/m^3	2770	5%
Added mass, kg	454.0	5%
A (element cross-section), cm^2	$A_1 = 42.893$, $A_2 = 19.020$, $A_3 = 45.926$, $A_4 = 18.729$, $A_5 = 0.661$, $A_6 = 5.714$, $A_7 = 30.599$, $A_8 = 30.019$, $A_9 = 15.320$, $A_{10} = 15.883$	5%

```
for i=1:nWM
    Dist(i)=norm(WM(i,:)-worstWM);
end
[a,b]=sort(Dist);
for i=1:nWM/2
    droplet-WM(i,:)=WM(b(i),:);
end
Generate the corresponding θ vector and DEP matrix using Eqs. (10) and (11), respectively.
for i=1: nWM/2
    monolayer-WM(i,:)=WM(b(size(nWM/2+i),:);
end
Generate the corresponding E_sub vector and MEP matrix using Eqs. (8) and (9), respectively.
for i=1:size(WM,1)
    if i <= nWM/2
        MDEP(b(i),:)=DEP(i,:);
    else
        MDEP (b(i),:)=MEP(i-size(WM,1)/2,:);
    end
end
```

Fig. 2. Pseudo-code for constructing the **MDEP** matrix [31].

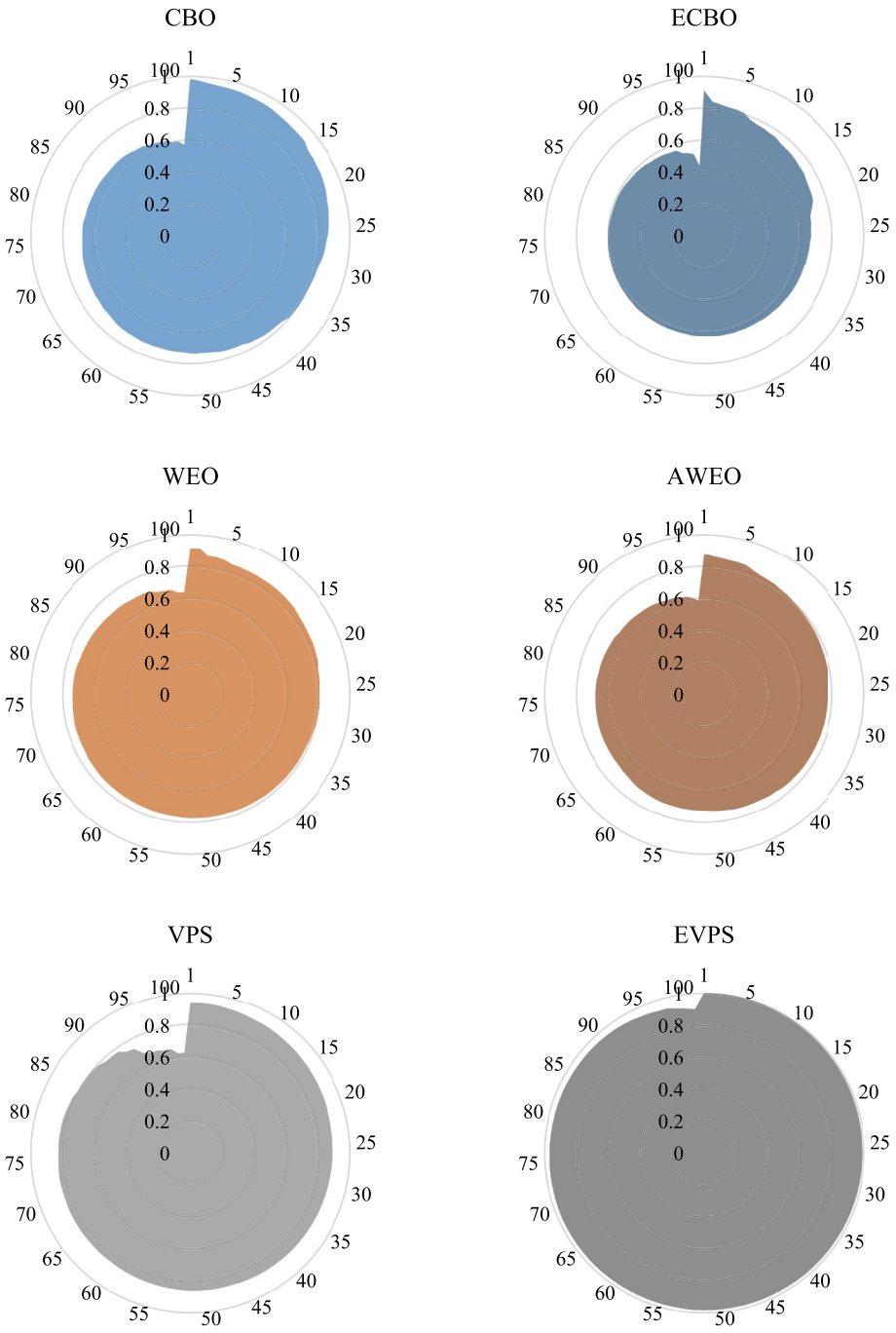

Fig. 4. Comparison of performance of algorithms in 100 independent runes for the 10-bar truss.

investigate the efficiency of the proposed approach for calculating the reliability index, the frequency limit of the first mode of the structure is selected as the probabilistic constraint. Accordingly, in Eq. (3), R is the value of the allowable frequency, ω_{all} in rad/s (f_{all} in Hz), which is mentioned in each problem separately. Also, Q indicate the value of the available frequency, ω in rad/s (f in Hz), in the truss structure. This parameter is obtained from modal analysis.

Avoiding the noise is impossible in real dynamic tests, and therefore the robustness of the proposed approach should be discussed. This issue is dealt with generating small deviation in experimental dynamic parameters (Eq. (7)) and the robustness of this approach has also been investigated for all problems.

$$\omega_{noise} = \omega \times (1 + \alpha \times Noise) \tag{7}$$

In Eq. (7), α is a random number in interval [-1, 1] and *Noise* is the deviations of the natural frequencies; ω_{noise} implies a frequency with noisy value.

3. Meta-heuristic optimization algorithms

3.1. Water evaporation optimization

The water evaporation optimization (WEO) algorithm has been proposed by Kaveh and Bakhshpouri [29] inspired by the process of evaporation of water molecules from the surface of solid objects at a microscopic scale and based on the equations presented by Wang et al. [30]. The WEO algorithm is consist of two distinct phases named monolayer evaporation and droplet.

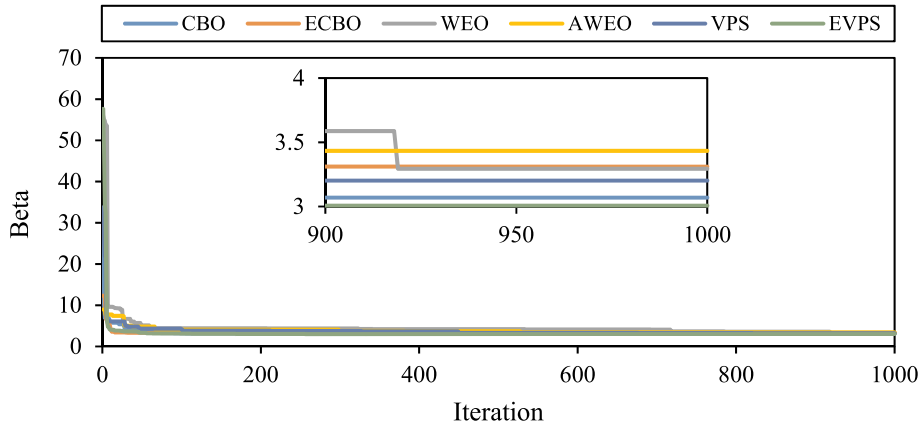

Fig. 5. Comparison of the convergence curves for the best run obtained by the algorithms for the 10-bar truss.

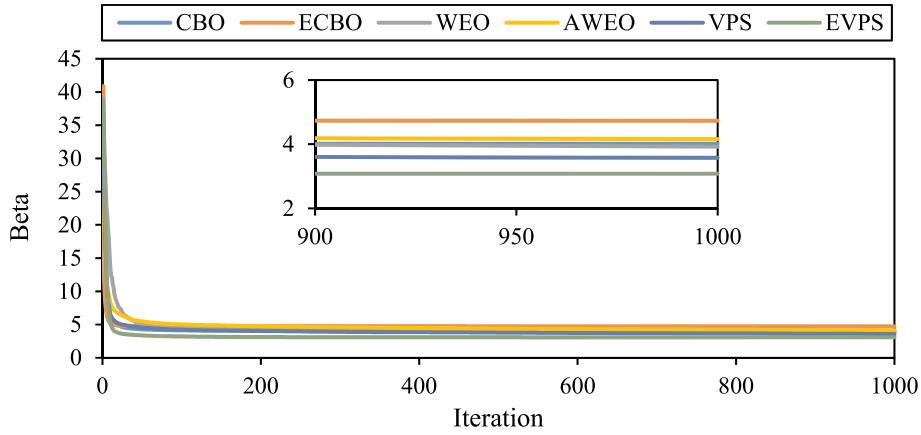

Fig. 6. Comparison of the convergence curves for the average runs obtained by the algorithms for the 10-bar truss.

Table 2
Statistical optimization results obtained by algorithms for the 10-bar truss problem.

	CBO	ECBO	WEO	AWEO	VPS	EVPS	MCS
Best β	3.0693	3.3110	3.2941	3.4335	3.2021	3.0067	-
Best β[a]	3.0754	3.3454	3.3278	3.4627	3.2118	3.0083	-
Worst β	5.2835	6.8397	4.7583	5.1457	4.8325	3.3376	-
Worst β[a]	5.5920	6.9753	4.9933	5.1828	4.8752	3.4185	-
Average β	4.0146	4.7317	3.9226	4.1588	3.5763	3.0790	2.9633
Average β[a]	4.2088	4.7622	3.9865	4.1902	3.5830	3.0958	-
Std β	0.5610	0.5346	0.2930	0.3720	0.3359	0.0641	0.0197
Std β[a]	0.5828	0.5464	0.3069	0.4193	0.3537	0.0883	-
Processing time (Sec.)	3.66	3.60	3.37	3.46	4.58	3.83	15.30
Total number of limit state function evaluations	3×10^4	3×10^4	3×10^4	3×10^4	3×10^4	3×10^4	2×10^5

[a] with considering noise.

The monolayer evaporation phase is performed in the first half of the optimization iterations ($t \leq t_{max}/2$). In this phase, the amount of substrate energy for the ith water molecule in the tth iteration (E_{sub} (i)^t) is calculated based on the value of the objective function (Fit_i^t) according to Eq. (8).

$$E_{sub}(i)^t = \frac{(E_{\max} - E_{\min}) \times \left(Fit_i^t - Min(Fit)\right)}{(Max(Fit) - Min(Fit))} + E_{\min} \tag{8}$$

In Eq. (8), $E_{\max}$ and $E_{\min}$ are respectively -0.5 and -3.5. $Max(Fit)$ and $Min(Fit)$ are the maximum and minimum values of the objective function of water molecules, respectively. After calculation of E_{sub} (i), monolayer evaporation probability (MEP) obtains according to Eq. (9).

$$MEP_{ij}^t = \begin{cases} 1 & \text{if } rand_{ij} < \exp(E_{sub}(i)^t) \\ 0 & \text{if } rand_{ij} \geq \exp(E_{sub}(i)^t) \end{cases} \tag{9}$$

In this equation, MEP_{ij}^t is the probability of updating the jth variable of ith water molecule in tth iteration.

The second phase is the droplet evaporation phase which is performed in the second half of optimization iterations ($t > t_{max}/2$). In this phase, the angle contact of ith water molecule in the tth iteration (θ_{sub} (i)^t) is defined based on the value of its objective function (Fit_i^t) according to Eq. (10).

$$\theta(i)^t = \frac{(\theta_{\max} - \theta_{\min}) \times \left(Fit_i^t - Min(Fit)\right)}{(Max(Fit) - Min(Fit))} + \theta_{\min} \tag{10}$$

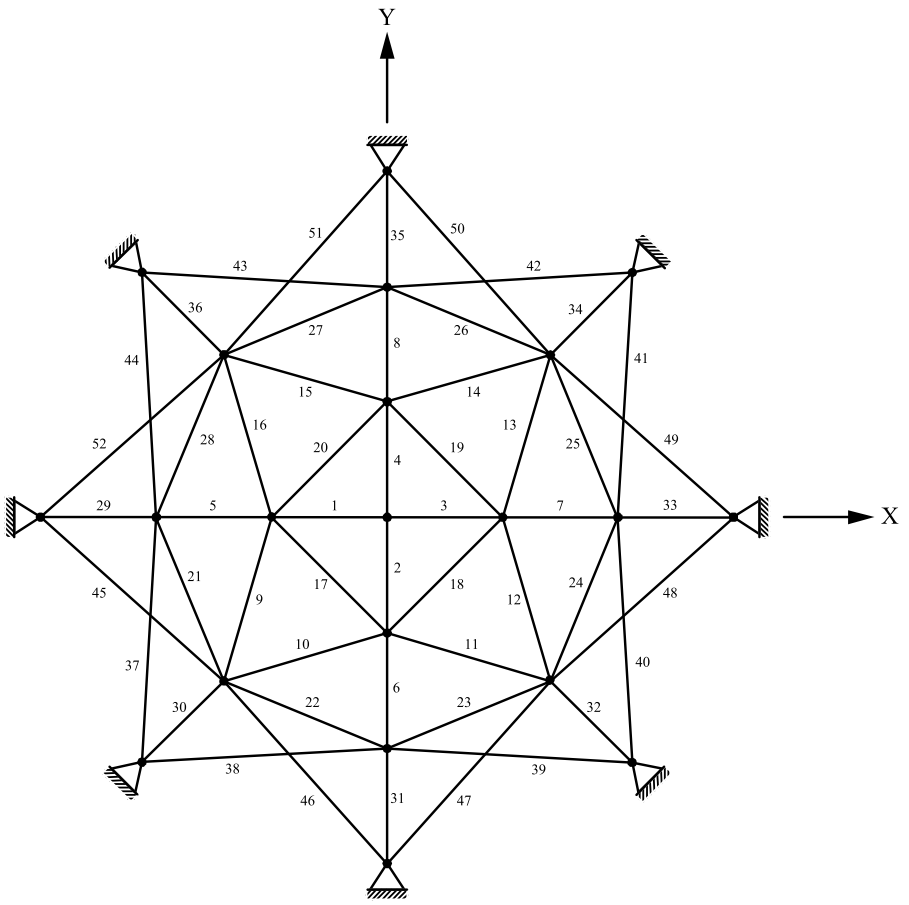

(a) Top view

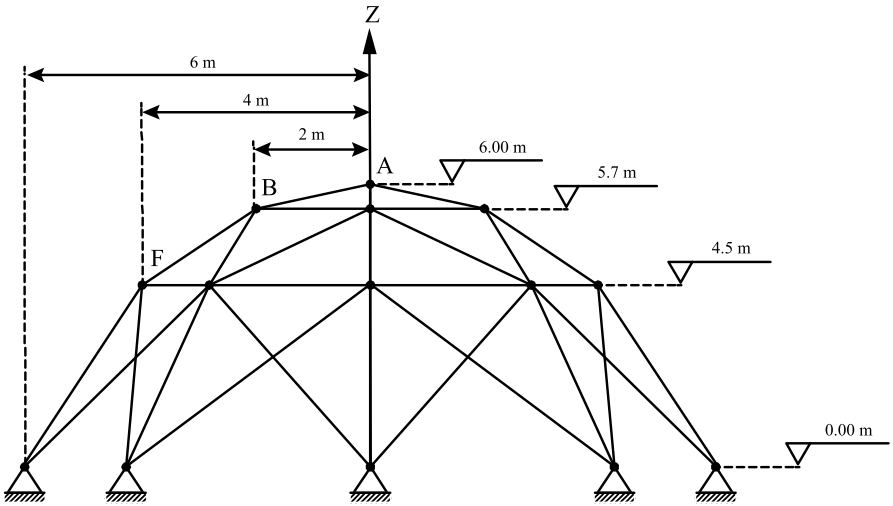

(b) Side view

Fig. 7. Schematic of the 52-bar dome-like truss.

In Eq. (10), θ_{max} and θ_{min} are -20° and -50°, respectively. Droplet evaporation probability (DEP) calculates according to Eq. (11).

$$DEP_{ij}^{t} = \begin{cases} 1 & \text{if } rand_{ij} < J\left(\theta_i^{(t)}\right) \\ 0 & \text{if } rand_{ij} \geq J\left(\theta_i^{(t)}\right) \end{cases} \quad (11)$$

In this equation, DEP_{ij}^{t} is updating the probability of the jth variable from ith water molecule in tth iteration; J is evaporation flow which is calculated according to Eq. (12) and its maximum and minimum values are 1.0 and 0.6, respectively.

Table 3
Element grouping adopted in the 52-bar dome-like truss problem.

Group number	Elements	Group number	Elements
1	1–4	5	21–28
2	5–8	6	29–36
3	9–16	7	37–44
4	17–20	8	45–52

Table 4
Random variables for the 52-bar dome-like truss problem.

Random Variable, unit	Mean	COV
E (Modulus of elasticity), N/m^2	2.1×10^{11}	5%
ρ (Material density), kg/m^3	7800	5%
Added mass, kg	50.0	5%
A (element group cross-section), cm^2	$A_1 = 1.0464$, $A_2 = 1.7295$, $A_3 = 1.6507$, $A_4 = 1.5059$, $A_5 = 1.7210$, $A_6 = 1.0020$, $A_7 = 1.7415$, $A_8 = 1.2555$	5%

$$J(\theta) = J_0 P_0 \left(\frac{2}{3} + \frac{\cos^3\theta}{3} - \cos\theta\right)^{-2/3} (1 - \cos\theta), \qquad J_0 P_0 = \frac{1}{2.6} \tag{12}$$

In both phases, random permutation is generated according to Eq. (13).

$$S = rand.(WM^{(t)}[permute1(i)(j)] - WM^{(t)}[permute2(i)(j)]) \tag{13}$$

In Eq. (13), *permute*1 and *permute*2 are two different rows of permutation functions; i indicates the number of water molecule and j is the number of the variable. $\mathbf{WM}^{(t)}$ is matrix of the position of input water molecules in tth iteration.

The position of the evaporated molecules ($\mathbf{WM}^{(t+1)}$) based on the current position of the water molecules ($\mathbf{WM}^{(t)}$) and evaporation probability matrices, is calculated according to Eq. (14). The sign "$\circ$" denotes an element-by-element multiplication.

$$WM^{(t+1)} = WM^{(t)} + S \circ \begin{cases} MEP^{(t)} & t \le t_{\max}/2 \\ DEP^{(t)} & t > t_{\max}/2 \end{cases} \tag{14}$$

If the value of the objective function of each evaporated molecule ($\mathbf{WM}^{(t+1)}$) is better than the objective function of the current water molecule ($\mathbf{WM}^{(t)}$), the current water molecule is replaced by the evaporated molecule. Otherwise, there is no change in the current water molecule. The best water molecule found so far has been stored and reported.

3.2. Accelerated water evaporation optimization

Accelerated water evaporation optimization (AWEO) algorithm is a version of WEO presented by Kaveh and Bakhshpouri [31]. As noted, WEO algorithm process takes place in two distinct phases; in other words, half of the optimization process is performed according to the monolayer evaporation phase and the other half according to droplet evaporation phase. However, in the process of AWEO algorithm, these two phases are used simultaneously in each iteration.

In each iteration of this algorithm, first, the vector of the distance between all the molecules and the worst current molecule (dist) is calculated according to Eq. (15).

$$dist_i = |worstWM - WM_i| \qquad (i = 1,\ 2,\ \ldots,\ nWM) \tag{15}$$

All molecules are sorted in an ascending order according to dist. Then, the MEP and DEP matrices are produced according to Eqs. (9) and (11) in order to update the first and second halves of the sorted molecules. **MDEP** matrix is formed by the combination of MEP and DEP matrices based on the pseudo-code shown in Fig. 2. After generating random permutations according to Eq. (13), the position of evaporated molecules ($\mathbf{WM}^{(t+1)}$) is calculated based on the current position of water molecules ($\mathbf{WM}^{(t)}$) and **MDEP** matrix according to Eq. (16).

$$WM^{(t+1)} = WM^{(t)} + S \circ MDEP^{(t)} \tag{16}$$

If the value of the objective function of each evaporated molecule ($\mathbf{WM}^{(t+1)}$) is better than the objective function of the current water molecule ($\mathbf{WM}^{(t)}$), the current water molecule is replaced by the evaporated molecule. Otherwise, there is no change in the current water molecule.

3.3. Colliding bodies optimization

Colliding bodies optimization (CBO) algorithm was proposed by Kaveh and Mahdavi inspired by the physical laws governing colliding bodies [32]. In each iteration of this algorithm, mass is first defined for all population (CBs) according to Eq. (17).

$$m_k = \left(\frac{1}{fit(k)}\right) \Big/ \left(\sum_{i=1}^{nCB} \frac{1}{fit(i)}\right) \tag{17}$$

In this equation, $fit(i)$ is the objective function of the ith colliding body (CB), and nCB is the number of algorithm population. After ascending sorting of the population based on the value of the objective function, the sorted population is divided into two equal groups: the first half of the population consists of stationary CBs and the second half includes moving CBs. The moving CBs move toward the stationary CBs and collide with them. The velocities before collision (v) and after collision of these two groups (v') calculate according to Eqs. (18) and (19):

$$v_i = \begin{cases} 0 & , \quad \left(i = 1,\ 2,\ \ldots,\ \dfrac{nCB}{2}\right) \\ x_i - x_{i-(nCB/2)} & , \quad \left(i = \dfrac{nCB}{2} + 1,\ \dfrac{nCB}{2} + 2,\ \ldots,\ nCB\right) \end{cases} \tag{18}$$

$$v'_i = \begin{cases} \left(\dfrac{m_{i+(nCB/2)} + \varepsilon m_{i+(nCB/2)}}{m_i + m_{i+(nCB/2)}}\right) v_{i+(nCB/2)} & , \quad \left(i = 1, 2, \ldots, \dfrac{nCB}{2}\right) \\ \left(\dfrac{m_i - \varepsilon m_{i-(nCB/2)}}{m_i + m_{i-(nCB/2)}}\right) v_i & , \quad \left(i = \dfrac{nCB}{2} + 1, \dfrac{nCB}{2} + 2, \ldots, nCB\right) \end{cases} \tag{19}$$

In this equations, v_i, v_i', x_i and m_i are respectively the velocities before and after collision, the position of the ith CB, and its mass. Parameter ε indicates the coefficient of restitution which is calculated by the following equation:

$$\varepsilon = 1 - \frac{t}{t_{\max}} \tag{20}$$

where t is the number of iteration and $t_{\max}$ is the total number of algorithm iterations.

The new position of the stationary and moving CBs will be obtained according to Eqs. (21) and (22):

$$x_i^{new} = x_i + rand \circ v'_i, \qquad \left(i = 1,\ 2,\ \ldots,\ \frac{nCB}{2}\right) \tag{21}$$

$$x_i^{new} = x_{i-(nCB/2)} + rand \circ v'_i, \qquad \left(i = \frac{nCB}{2} + 1,\ \frac{nCB}{2} + 2,\ \ldots,\ nCB\right) \tag{22}$$

In this equations, x_i is the current position of the ith CB, and *rand* represents a vector with a dimension of the number of problem variables (N) consisting of random numbers in the interval (-1, 1).

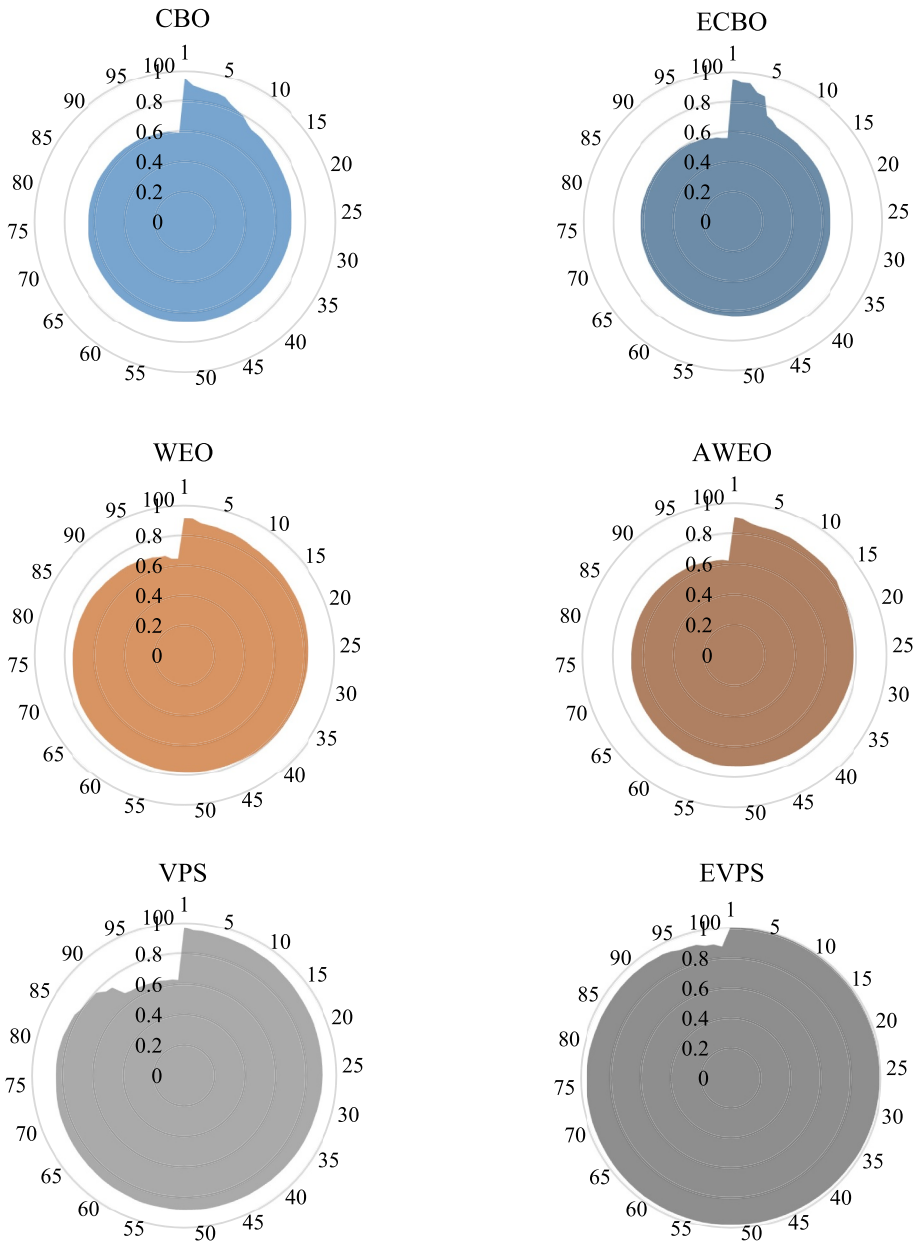

Fig. 8. Comparison of performance of algorithms in 100 independent runes for the 52-bar truss.

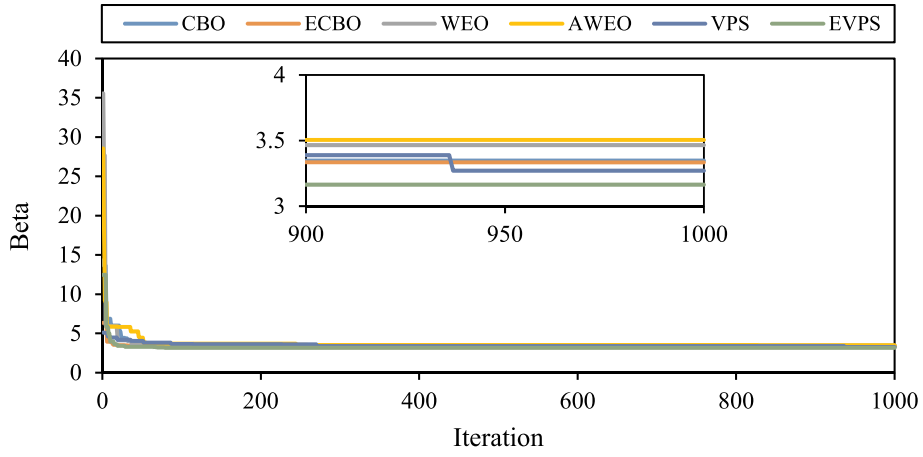

Fig. 9. Comparison of the convergence curves for the best run obtained by the algorithms for the 52-bar truss.

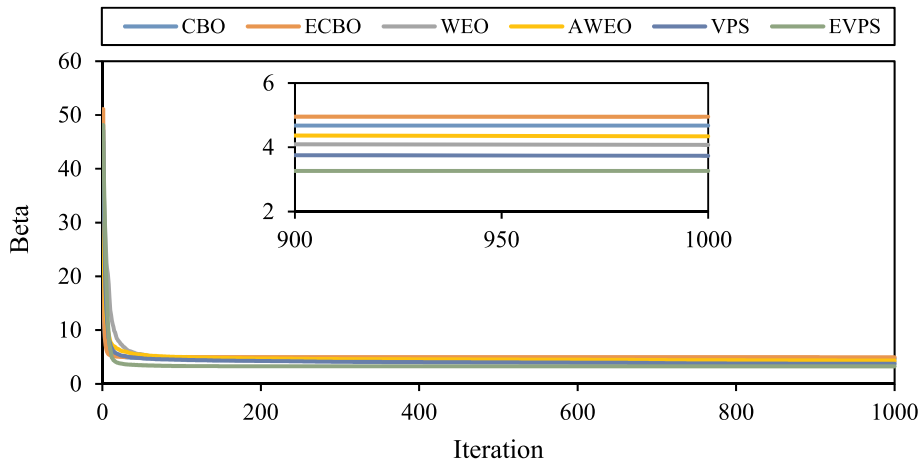

Fig. 10. Comparison of the convergence curves for the average runs obtained by the algorithms for the 52-bar truss.

Table 5
Statistical optimization results obtained by algorithms for the 52-bar truss problem.

	CBO	ECBO	WEO	AWEO	VPS	EVPS	MCS
Best β	3.3472	3.3335	3.4648	3.5046	3.2701	3.1635	-
Best β[a]	3.3658	3.3582	3.4699	3.5667	3.3050	3.1654	-
Worst β	5.4004	5.6919	4.9194	5.1142	5.0806	3.6287	-
Worst β[a]	5.6611	5.9002	4.9285	5.2385	5.1260	3.7460	-
Average β	4.6761	4.9533	4.0739	4.3435	3.7334	3.2652	3.1303
Average β[a]	4.6929	4.9892	4.1025	4.3676	3.7715	3.2757	-
Std β	0.4126	0.4127	0.3043	0.3966	0.4418	0.0927	0.0208
Std β[a]	0.4888	0.4179	0.3116	0.4468	0.4578	0.1044	-
Processing time (Sec.)	28.96	28.28	28.19	28.48	29.18	28.49	177.43
Total number of limit state function evaluations	3×10^4	3×10^4	3×10^4	3×10^4	3×10^4	3×10^4	2×10^5

[a] with considering noise.

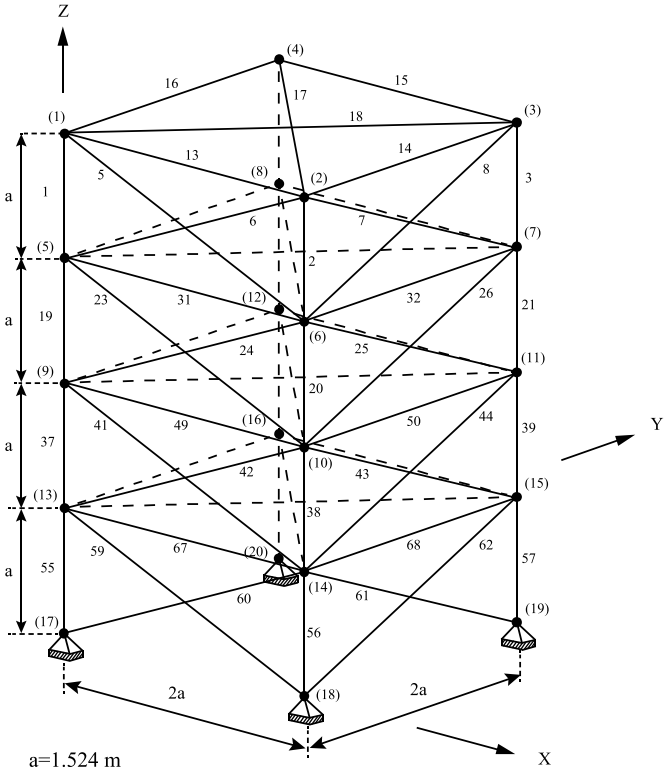

Fig. 11. Schematic of the 72-bar transmission truss.

Table 6
Element grouping and their sections in the 72-bar transmission truss problem.

Group number	Elements	Cross-sectional areas (cm^2)	Group number	Elements	Cross-sectional areas (cm^2)
1	1–4	2.987	9	37–40	13.450
2	5–12	7.849	10	41–48	8.073
3	13–16	0.645	11	49–52	0.645
4	17–18	0.645	12	53–54	0.645
5	19–22	8.765	13	55–58	16.684
6	23–30	8.153	14	59–66	8.159
7	31–34	0.645	15	67–70	0.645
8	35–36	0.645	16	71–72	0.645

Table 7
Random variables for the 72-bar transmission truss problem.

Random Variable, unit	Mean	COV
E (Modulus of elasticity), N/m^2	6.98×10^{10}	5%
ρ (Material density), kg/m^3	2770.0	5%
Added mass, kg	2270.0	5%
A (element group cross-section), cm^2	Mentioned in Table 6	5%

3.4. Enhanced colliding bodies optimization

Enhanced colliding bodies optimization (ECBO) algorithm was introduced by Kaveh and Ilchi Ghazaan in order to improve the CBO performance [33]. This algorithm uses memory to enhance the convergence rate of the CBO algorithm. Accordingly, in each iteration of the algorithm, n best answers found are saved in the colliding memory (CM). These answers are added to the population and n worst members

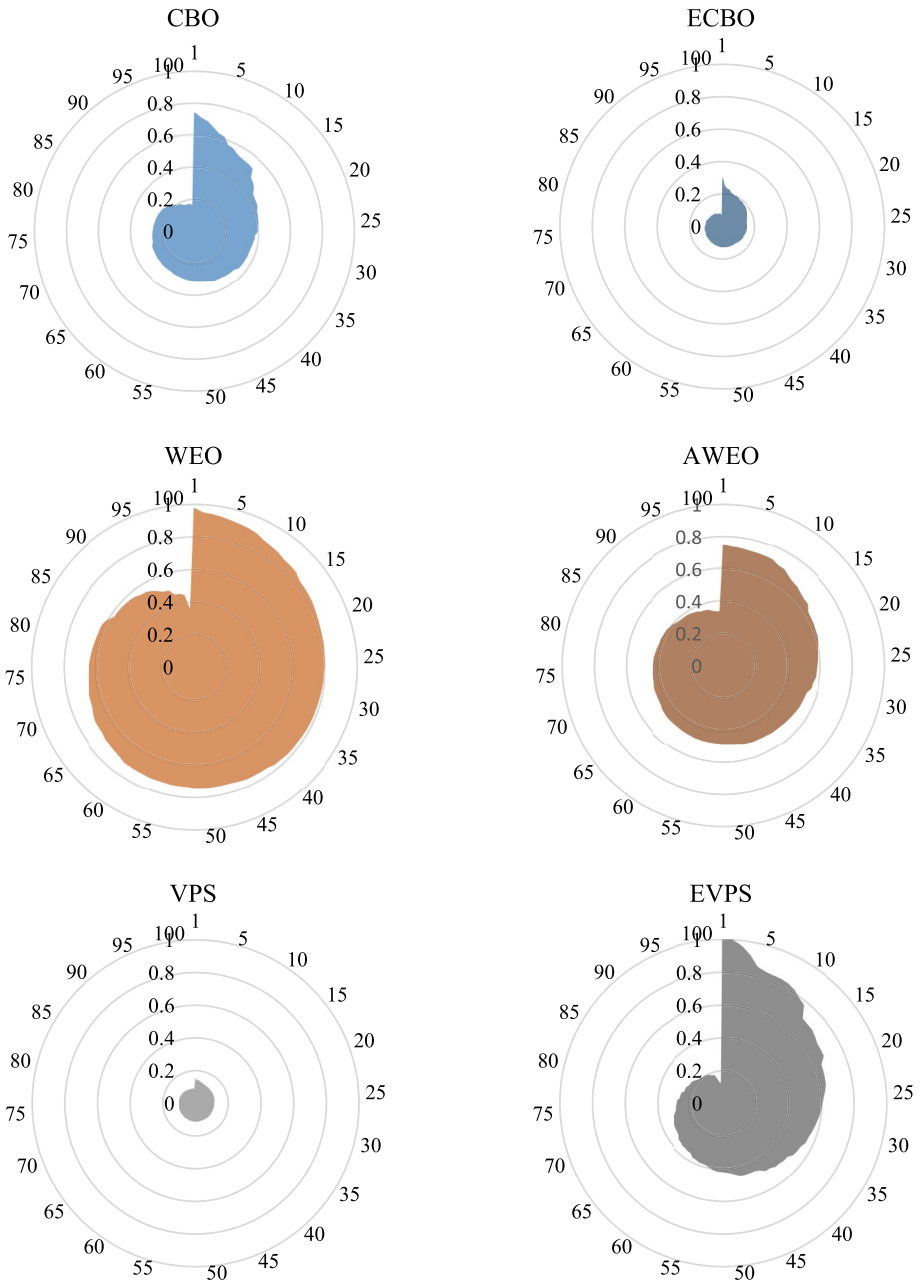

Fig. 12. Comparison of performance of algorithms in 100 independent runes for the 72-bar truss.

of the current population are eliminated. Then the new population is sorted in an ascending order according to the values of their objective function. Finally, the new position of moving and stationary CBs is calculated similar to CBO algorithm. Also, a parameter called *Pro* is defined in the interval (0, 1) in order to accelerate escape from local optima. For each variable of every CB, the value of *Pro* is compared with rn_j ($j = 1, 2, \ldots, N$) which is a random number in interval (0, 1). If rn_j is smaller than *Pro*, the *j*th variable of the considered CB will be generated randomly.

3.5. Vibrating particles system algorithm

Vibrating particles system (VPS) algorithm was proposed by Kaveh and Ilchi Ghazaan based on the free vibration of freedom systems single degree with viscous damping [34]. In this algorithm, the position of each particle is updated according to the following three positions with different relative importance:

- *HB*: The best position found for all particles;
- *GP*: A good particle that is randomly selected from the first half of the population sorted based on increased value of the objective function in each iteration;
- *BP*: A bad particle that is randomly selected from the second half of the population sorted based on increased value of the objective function in each iteration.

The position of each particle is updated according to Eq. (23).

$$\begin{aligned} x_i^j = {} & \omega_1.\left[D.A.rand1.HB^j\right] + \omega_2.\left[D.A.rand2.GP^j\right] \\ & + \omega_3.\left[D.A.rand3.BP^j\right] A = \left[\omega_1.\left(HB^j - x_i^j\right)\right] + \left[\omega_2.\left(GP^j - x_i^j\right)\right] \\ & + \left[\omega_3.\left(BP^j - x_i^j\right)\right] \omega_1 + \omega_2 + \omega_3 = 1 \end{aligned} \tag{23}$$

In Eq. (22), $x_i{}^j$ is the value of the *j*th variable of the *i*th particle; *rand*1, *rand*2, and *rand*3 are random numbers in interval [0, 1]; ω_1, ω_2 and ω_3 are parameters which define the relative importance of *HB*, *GP*, and *BP*,

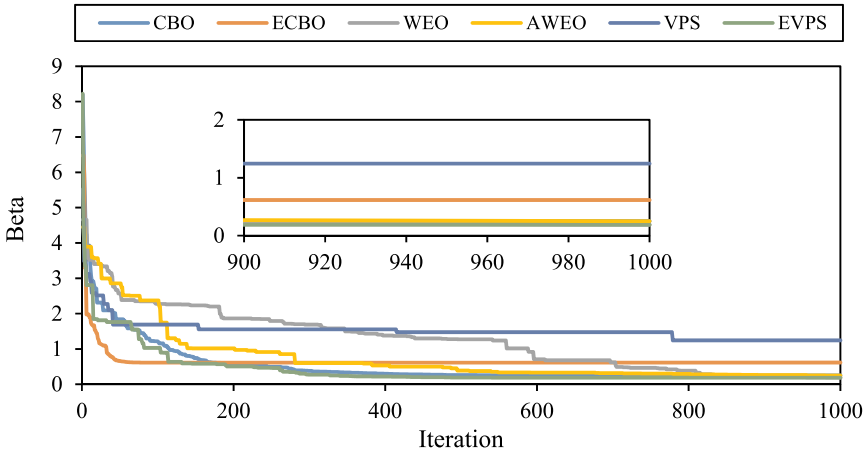

Fig. 13. Comparison of the convergence curves for the best run obtained by the algorithms for the 72-bar truss.

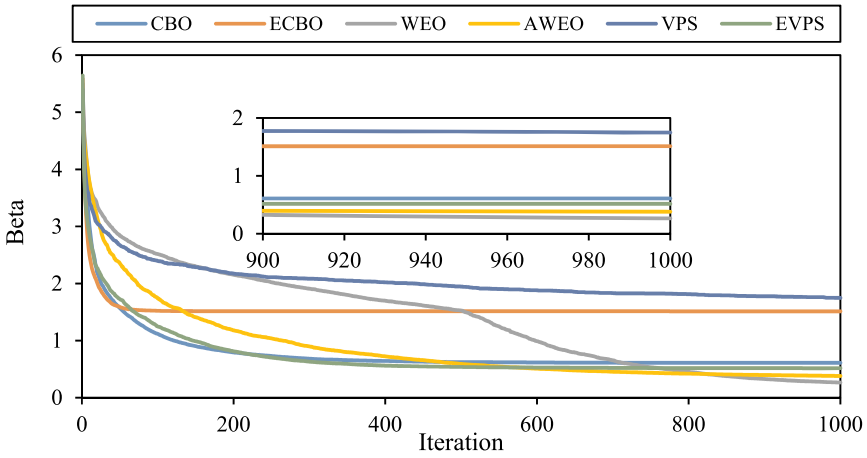

Fig. 14. Comparison of the convergence curves for the average runs obtained by the algorithms for the 72-bar truss.

Table 8
Statistical optimization results obtained by algorithms for the 72-bar truss problem.

	CBO	ECBO	WEO	AWEO	VPS	EVPS	MCS
Best β	0.2511	0.6147	0.1898	0.2489	1.2434	0.1856	-
Best β[a]	0.2669	0.8146	0.1914	0.2539	1.2448	0.1958	-
Worst β	1.1271	2.6767	0.5177	0.5565	2.2151	1.4904	-
Worst β[a]	1.2763	2.7008	0.5521	0.5786	2.2422	1.6689	-
Average β	0.6100	1.5122	0.2653	0.3803	1.7480	0.5165	0.1452
Average β[a]	0.6105	1.6110	0.2662	0.3806	1.7583	0.5339	-
Std β	0.2027	0.3974	0.0545	0.0773	0.1894	0.2749	0.0027
Std β[a]	0.2395	0.4018	0.0557	0.0795	0.1903	0.2768	-
Processing time (Sec.)	37.02	36.64	36.07	36.49	36.35	36.09	220.49
Total number of limit state function evaluations	3×10^4	3×10^4	3×10^4	3×10^4	3×10^4	3×10^4	2×10^5

[a] with considering noise.

respectively; and D is parameter of damping surface modeling in vibration, which is defined according to Eq. (24).

$$D = \left(\frac{t}{t_{\max}}\right)^{\alpha} \tag{24}$$

In this equation, t is the current iteration; $t_{\max}$ is the maximum iteration of optimization process; and α is a constant value.

Also, parameter p is defined for each particle in interval (0, 1) in order to accelerate convergence process. If p is smaller than a random number in the interval [0, 1], ω_3 will be considered to be zero.

3.6. Enhanced Vibrating Particles System

Enhanced Vibrating Particles System (EVPS) algorithm was presented by Kaveh et al. in order to improve VPS performance [35]. In this algorithm, OHB replaces HB by enhancing the memory which stores NB best total positions. OHB is one of memory positions which is selected randomly (OHB, GP, and BP are obtained independently for each particle). Moreover, the particle position is updated according to one of the equations (*a*), (*b*), or (*c*) in Eq. (25) with probability of ω_1, ω_2 and ω_3, respectively. In this equation, *rand* is a random number in the interval [0, 1].

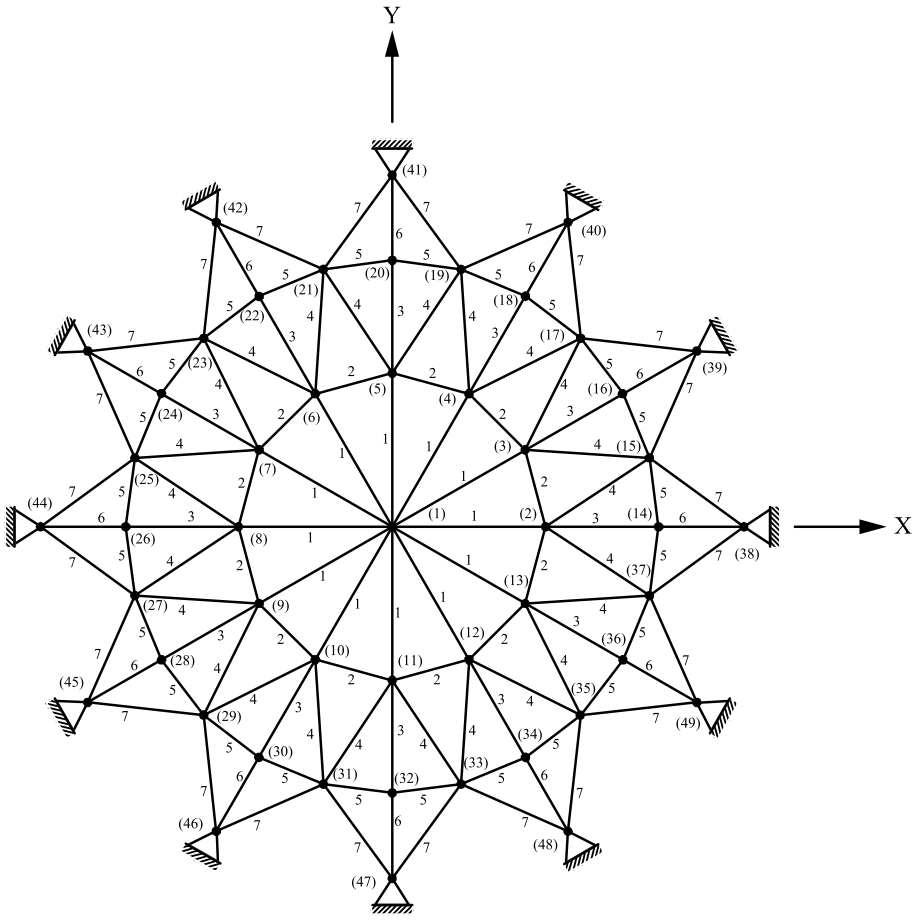

(a) Top view

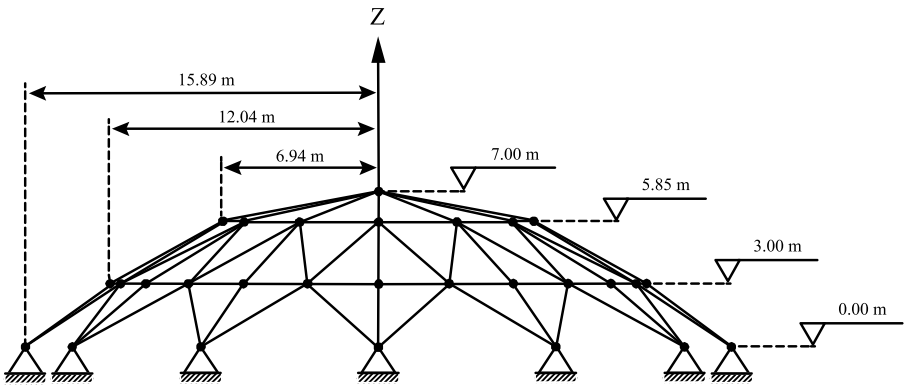

(b) Side view

Fig. 15. Schematic of the 120-bar dome truss.

$$x_i^j = \begin{cases} [D.A.rand1.OHB^j] \\ [D.A.rand2.GP^j] \\ [D.A.rand3.BP^j] \end{cases} \quad A = \begin{cases} (-1)^{round(rand)}\left(OHB^j - x_i^j\right) & (a) \\ (-1)^{round(rand)}\left(GP^j - x_i^j\right) & (b) \quad \omega_1+\omega_2+\omega_3=1 \\ (-1)^{round(rand)}\left(BP^j - x_i^j\right) & (c) \end{cases} \tag{25}$$

4. Numerical problems

In this section, the reliability indices of four benchmark trusses optimized by other researchers has been calculated using the proposed meta-heuristic algorithms and the results are presented. The reliability index in all problems is for the frequency constraint of the first mode (ω_1). Random variables considered in all problems include: modulus of elasticity (E), mass per unit volume (ρ), the value of non-structural mass, and cross-section of the elements or elements group. All random variables have a normal distribution with a coefficient of variation of 5%. To ensure algorithms performance, the reliability index for each of the problems (with and without noise) obtained in 100 independent runs by each of the algorithms. For all problems, the number of considered population and iterations of all algorithms are 30 and 1000,

Table 9
Random variables for the 120-bar dome truss problem.

Random Variable, unit	Mean	COV
E (Modulus of elasticity), N/m^2	2.1×10^{11}	5%
ρ (Material density), kg/m^3	7971.810	5%
Added mass, kg	$m_1 = 3000$, $m_2 = 500$, $m_3 = 100$	5%
A (element group cross-section), cm^2	$A_1 = 19.523$, $A_2 = 97.161$, $A_3 = 30.368$, $A_4 = 20.000$, $A_5 = 54.922$, $A_6 = 23.832$, $A_7 = 16.148$	5%

respectively. In all problems, number of considered samples (n) for each random variables and *Noise* are 10^6 and 0.05, respectively. In order to evaluate accuracy of the algorithms performance in calculating the reliability index, the MCS method with 2×10^5 samples is used for all problems. A system with a Core i7-6700 4.00 GHz CPU is employed for computer implementation, and the computational time is measured in terms of CPU time.

4.1. A 10-bar planar truss

The first considered problem is the 10-bar truss shown in Fig. 3. This truss is a well-known benchmark problem which has been studied by many researchers [36–39]. Non-structural mass of 454.0 kg has been added to free nodes. The cross-section of the elements is selected according to the optimal design of V. Ho-Huu et al. [40]. Characteristics of this problem are shown in Table 1. There are 13 random variables in this problem. Probabilistic constraint considered for this truss is $\omega_1 \geq 43.9823$ rad/s ($f_1 \geq 7.0$ Hz) which the reliability index calculated based on it.

Fig. 4 shows the performance of algorithms relative to each other in 100 independent runs. The charts indicate the ratio of the best overall solution to the solution of each run in an ascending order for each algorithm. The higher the ratio, the lower the difference between the best solution and the solutions obtained from the runs and consequently, the better solution. According to the figure, EVPS algorithm has a more uniform performance than other algorithms. Figs. 5 and 6 show the convergence process of the best solution and average responses of each algorithm. Table 2 reports the results of algorithms for this problem (the best, the worst, and average solutions of each algorithm) and the reliability index value calculated from the MCS method. This table shows that the EVPS algorithm has been able to find the best solution with an admissible difference with the value obtained from the MCS method. By comparing the amount of β and β^a, the robustness of this approach to noisy values of frequency is approved.

4.2. A 52-bar dome-like truss

The 52-bar dome-like truss has been considered as the second problem. The geometry of this truss is shown in Fig. 7. This truss is studied in the optimization literature as a problem for optimizing the shape and size of cross-section of elements under the frequency constraint [41–43]. The elements of this truss are divided into 8 groups according to Table 3. The cross-section of the elements group is selected according to the optimal design of Kaveh and Zolghadr [44]. Characteristics of materials and the amount of nonstructural mass added to all free nodes of the 52-bar truss are shown in Table 4. There are 11 random variables in this problem. Probabilistic constraint considered for this truss is $\omega_1 \leq 100.2859$ rad/s ($f_1 \leq 15.961$ Hz).

Fig. 8 shows the performance of algorithms relative to each other in 100 independent runs. According to this figure, EVPS algorithm has a more uniform performance than other algorithms. Figs. 9 and 10 indicate the convergence process of the best solution and average solutions of each algorithm. Table 5 reports the best, the worst, and average solutions of each algorithm as well as the reliability index value obtained from the MCS method. This table shows that the ability of EVPS algorithm to find the best optimal solution (calculation of reliability index) is higher than other algorithms for this problem, an answer with an acceptable difference with the answer of MCS method has been found. Also, the robustness of proposed approach to noisy values of frequency is verified by comparing the amount of β and β^a.

4.3. A 72-bar transmission truss

The 72-bar transmission truss which is indicated in Fig. 11 is the third structure that its reliability index is calculated using meta-heuristic algorithms. The 72-bar truss is a famous problem in the field of optimization [35,45–47]. The 72 elements of this truss are divided into 16 groups whose cross-sectional area has been selected based on Gomes optimal design [48]. Grouping of the elements and their cross-sections are specified in Table 6. Nodes 1 to 4 have been assigned 2270 kg of non-structural mass. Structural characteristics and frequency constraint of the 72-bar truss are indicated in Table 7. There are 19 random variables in this problem. Probabilistic constraint considered for this truss is $\omega_1 \geq 25.1327$ rad/s ($f_1 \geq 4.0$ Hz).

The performance of algorithms relative to each other in 100 independent runs is shown in Fig. 12. According to this figure, the performance of WEO algorithm is more uniform and appropriate relative to other algorithms in this problem. The convergence process of the best solution and average solutions of each algorithm are shown in Figs. 13 and 14, respectively. The best, the worst, average solutions of each algorithm and the reliability index value calculated from the MCS method for this problem is reported in Table 8. This table shows that EVPS algorithm has been able to find the best answer with an acceptable difference with the answer of MCS method. By comparing the amount of β and β^a, the robustness of proposed approach to noisy values of frequency is confirmed.

4.4. A 120-bar dome truss

The last studied problem is 120-bar dome truss. Many researchers

Table 10
Statistical optimization results obtained by algorithms for the 120-bar truss problem.

	CBO	ECBO	WEO	AWEO	VPS	EVPS	MCS
Best β	2.7453	2.7960	2.9963	3.0951	2.8245	2.6925	-
Best β^a	2.7470	2.8346	3.0142	3.1258	2.8882	2.6960	-
Worst β	5.5608	6.8707	4.3238	4.9215	3.6531	3.8895	-
Worst β^a	5.8994	6.8965	4.4868	4.9987	3.8337	3.9843	-
Average β	3.6679	4.4132	3.6879	3.7516	3.1780	2.8016	2.6436
Average β^a	3.8807	4.4561	3.6956	3.7779	3.1848	2.8186	-
Std β	0.7926	0.9931	0.2996	0.3991	0.1612	0.1414	0.0114
Std β^a	0.8116	0.9947	0.3122	0.4211	0.1837	0.1503	-
Processing time (Sec.)	71.80	72.64	71.31	71.42	72.36	71.69	462.78
Total number of limit state function evaluations	3×10^4	3×10^4	3×10^4	3×10^4	3×10^4	3×10^4	2×10^5

[a] with considering noise.

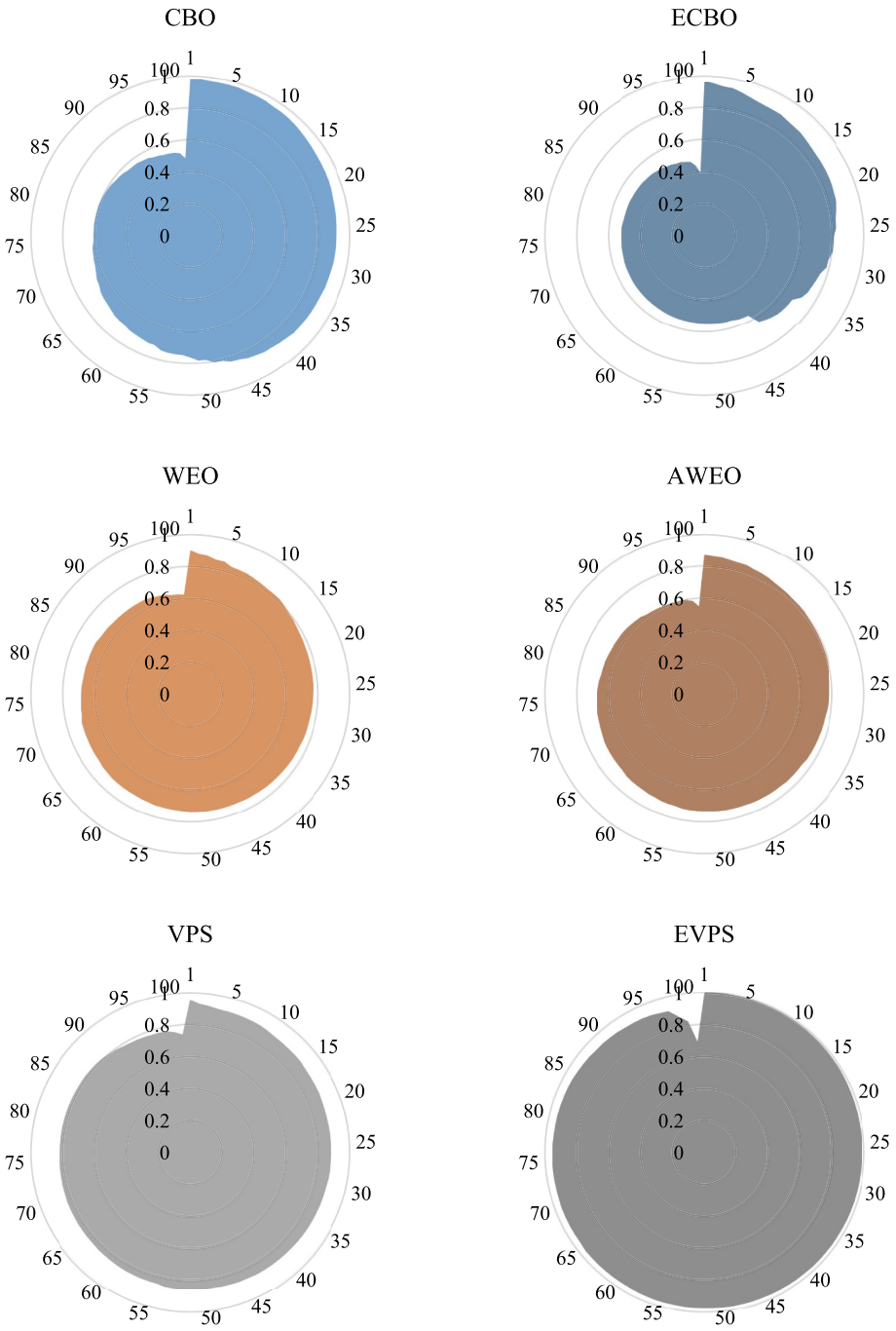

Fig. 16. Comparison of performance of algorithms in 100 independent runes for the 120-bar truss.

have optimized this truss [49–51]. The elements of this truss have been divided into 7 groups. Fig. 15 indicates the elements grouping and the geometry of the truss. Non-structural masses attached to Node 1 is $m_1 = 3000$ kg, nodes 2 to 13 are $m_2 = 500$ kg, and rest of the nodes are $m_3 = 100$ kg. Structural characteristics of this truss and the cross-section assigned to each elements group according to the optimal design of Kaveh et al. [52] are summarized in Table 9. There are 10 random variables in this problem. Reliability index considered for this truss is $\omega_1 \geq 56.54867$ rad/s ($f_1 \geq 9.0$ Hz).

The performance of the algorithms is compared to each other in 100 independent runs in Fig. 16. According to Fig. 16, the performance of EVPS algorithm in this problem is more uniform than other algorithms. Furthermore, the convergence process of the best solution and average solutions of each algorithm are shown in Figs. 17 and 18, respectively. Table 10 reports the best, the worst, and average solutions of each algorithm as well as the reliability index value obtained from the MCS method for this problem. This table shows that EVPS algorithm has been able to find the best solution with a suitable difference with the answer of MCS method. A comparison of the values of β and β^a shows the robustness of the proposed approach to noisy frequency values.

5. Conclusion

Parameters such as properties of materials and cross-section of members are statistically non-deterministic. Reliability theory is used to evaluate the uncertainty of these parameters. There are various methods to calculate the reliability index. Calculation of this index can be defined as an optimization problem. Hence, the use of meta-heuristic algorithms

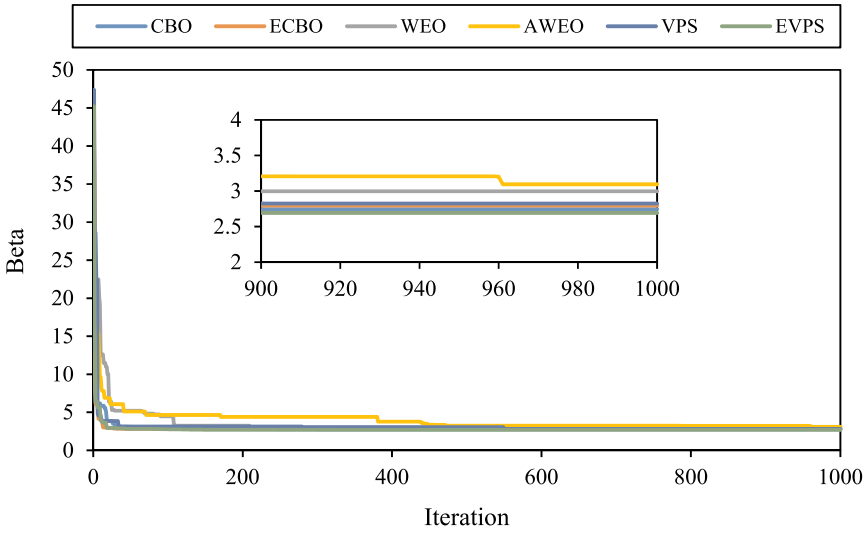

Fig. 17. Comparison of the convergence curves for the best run obtained by the algorithms for the 120-bar truss.

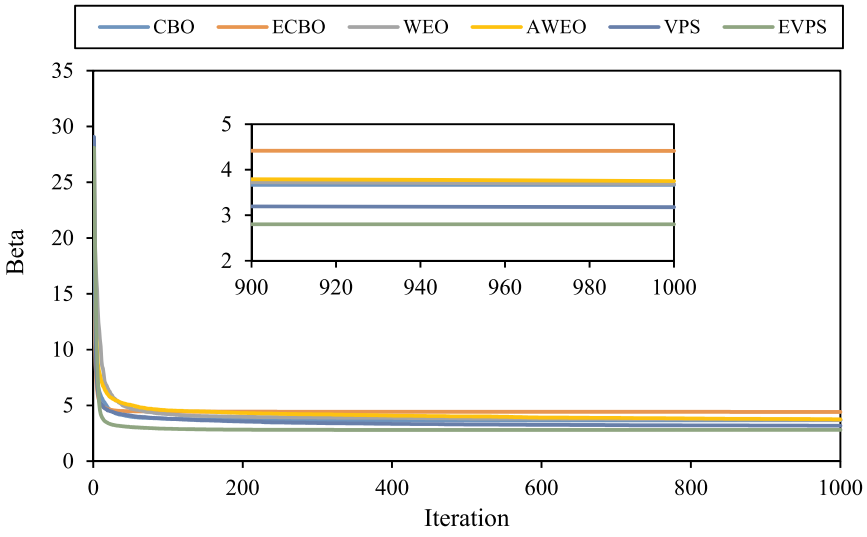

Fig. 18. Comparison of the convergence curves for the average runs obtained by the algorithms for the 120-bar truss.

can be used for calculating the reliability index. In structural reliability problems whose limit state function is not available in the form of explicit mathematical form, meta-heuristic algorithms less used. In this article, the reliability index of such problems is calculated using meta-heuristic algorithms. Accordingly, the reliability index calculation defined as the optimization problem. Then, to evaluate the ability of algorithms in structural reliability assessment, the reliability index of four truss structures with probabilistic constraint on first mode frequency was calculated and reported using WEO, AWEO, CBO, ECBO, VPS, and EVPS algorithms. The difference in the best solution of the algorithms for problems one through four with the value of reliability index calculated by the MCS method for each of the problems are respectively as follows: 0.043, 0.033, 0.040, and 0.049. These values and comparison of other results from the algorithms with the results of the MCS method show that the reliability index of the structures can be calculated with an acceptable accuracy and a lower processing time using the meta-heuristic algorithms. Also, by generating a small deviation in experimental dynamic parameters, the robustness of the proposed approach has been investigated and verified. Comparing the performance of algorithms demonstrates the proper and uniform performance of EVPS and WEO algorithms in calculation of the reliability index of the structures.

Declaration of competing interest

We wish to confirm that there are no known conflicts of interest associated with this publication. We confirm that the manuscript has been read and approved by all named authors and that there are no other persons who satisfied the criteria for authorship but are not listed. We further confirm that the order of authors listed in the manuscript has been approved by all of us.

References

[1] S.K. Mishra, B.K. Roy, S. Chakraborty, Reliability-based-design-optimization of base isolated buildings considering stochastic system parameters subjected to random earthquakes, Int. J. Mech. Sci. 75 (2013) 123–133.
[2] L. Wang, R.V. Grandhi, Safety index calculation using intervening variables for structural reliability analysis, Comput. Struct. 59 (1996) 1139–1148.
[3] C.A. Cornell, A probability-based structural code, J. Proc. (1969) 974–985.
[4] A.M. Hasofer, N.C. Lind, Exact and invariant second-moment code format, J. Eng. Mech. Div. 100 (1974) 111–121.

[5] Y.T. Wu, P.H. Wirsching, New algorithm for structural reliability estimation, J. Eng. Mech. 113 (1987) 1319–1336.
[6] Y.-G. Zhao, T. Ono, A general procedure for first/second-order reliability method (FORM/SORM), Struct. Saf. 21 (1999) 95–112.
[7] Y.-G. Zhao, T. Ono, Moment methods for structural reliability, Struct. Saf. 23 (2001) 47–75.
[8] S.H. Lee, B.M. Kwak, Response surface augmented moment method for efficient reliability analysis, Struct. Saf. 28 (2006) 261–272.
[9] E. Jahani, M.A. Shayanfar, M.A. Barkhordari, A new adaptive importance sampling Monte Carlo method for structural reliability, KSCE J. Civ. Eng. 17 (2013) 210–215.
[10] D.K. Green, Efficient Markov chain Monte Carlo for combined Subset Simulation and nonlinear finite element analysis, Comput. Methods Appl. Mech. Eng. 313 (2017) 337–361.
[11] G. Schueller, Efficient Monte Carlo simulation procedures in structural uncertainty and reliability analysis-recent advances, Struct. Eng. Mech. 32 (2009) 1–20.
[12] A. Naess, B. Leira, O. Batsevych, System reliability analysis by enhanced Monte Carlo simulation, Struct. Saf. 31 (2009) 349–355.
[13] M. Yonezawa, S. Okuda, H. Kobayashi, Structural reliability estimation based on quasi ideal importance sampling simulation, Struct. Eng. Mech. 32 (2009) 55–69.
[14] C. Bucher, Asymptotic sampling for high-dimensional reliability analysis, Probabilistic Eng. Mech. 24 (2009) 504–510.
[15] M. Rashki, M. Miri, M. Azhdary Moghaddam, A new efficient simulation method to approximate the probability of failure and most probable point, Struct. Saf. 39 (2012) 22–29.
[16] A. Kaveh, A. Dadras, An efficient method for reliability estimation using the combination of asymptotic sampling and weighted simulation, Sci. Iran. 26 (2019) 2108–2122.
[17] C. Elegbede, Structural reliability assessment based on particles swarm optimization, Struct. Saf. 27 (2005) 171–186.
[18] L. Deng, M. Ghosn, S. Shao, Development of a shredding genetic algorithm for structural reliability, Struct. Saf. 27 (2005) 113–131.
[19] D. Zou, L. Gao, J. Wu, S. Li, Y. Li, A novel global harmony search algorithm for reliability problems, Comput. Ind. Eng. 58 (2010) 307–316.
[20] D. Zou, L. Gao, S. Li, J. Wu, An effective global harmony search algorithm for reliability problems, Expert Syst. Appl. 38 (2011) 4642–4648.
[21] E. Valian, S. Tavakoli, S. Mohanna, A. Haghi, Improved cuckoo search for reliability optimization problems, Comput. Ind. Eng. 64 (2013) 459–468.
[22] A. Kaveh, M. Massoudi, M.G. Bagha, Structural reliability analysis using charged system search algorithm, Iran. J. Scui. Technol. Trans. Civ. Eng. 38 (2014) 439.
[23] A. Kaveh, M. Ilchi Ghazaan, Structural reliability assessment utilizing four metaheuristic algorithms, Int. J. Optim. Civ. Eng. 5 (2015) 205–225.
[24] A. Kaveh, S.R. Hoseini Vaez, P. Hosseini, Modified dolphin monitoring operator for weight optimization of frame structures, Period. Polytech. Civ. Eng. 61 (2017) 770–779.
[25] A. Kaveh, D. Jafarpour Laien, Optimal design of reinforced concrete cantilever retaining walls using CBO, ECBO and VPS algorithms, Asian J. Civ. Eng. 18 (2017) 657–671.
[26] A. Kaveh, S.R. Hoseini Vaez, P. Hosseini, Performance of the modified dolphin monitoring operator for weight optimization of skeletal structures, Period. Polytech. Civ. Eng. 63 (2019) 30–45.
[27] M.A. Fathali, S.R. Hoseini Vaez, Optimum performance-based design of eccentrically braced frames, Eng. Struct. 202 (2020), 109857.
[28] R. Rackwitz, B. Flessler, Structural reliability under combined random load sequences, Comput. Struct. 9 (1978) 489–494.
[29] A. Kaveh, T. Bakhshpoori, Water Evaporation Optimization: a novel physically inspired optimization algorithm, Comput. Struct. 167 (2016) 69–85.
[30] S. Wang, Y. Tu, R. Wan, H. Fang, Evaporation of tiny water aggregation on solid surfaces with different wetting properties, J. Phys. Chem. B 116 (2012) 13863–13867.
[31] A. Kaveh, T. Bakhshpoori, An accelerated water evaporation optimization formulation for discrete optimization of skeletal structures, Comput. Struct. 177 (2016) 218–228.
[32] A. Kaveh, V.R. Mahdavi, Colliding bodies optimization: a novel meta-heuristic method, Comput. Struct. 139 (2014) 18–27.
[33] A. Kaveh, M. Ilchi Ghazaan, Enhanced colliding bodies optimization for design problems with continuous and discrete variables, Adv. Eng. Software 77 (2014) 66–75.
[34] A. Kaveh, M. Ilchi Ghazaan, A new meta-heuristic algorithm: vibrating particles system, Sci. Iran. 24 (2017) 551–566.
[35] A. Kaveh, S.R. Hoseini Vaez, P. Hosseini, Enhanced vibrating particles system algorithm for damage identification of truss structures Scientia, Iranica 26 (2019) 246–256.
[36] G.G. Tejani, V.J. Savsani, V.K. Patel, S. Mirjalili, Truss optimization with natural frequency bounds using improved symbiotic organisms search, Knowl. Based Syst. 143 (2018) 162–178.
[37] M. Kooshkbaghi, A. Kaveh, Sizing optimization of truss structures with continuous variables by artificial coronary circulation system Algorithm, Iran. J. Sci. Technol. Trans. Civ. Eng. (2019). https://doi.org/10.1007/s40996-019-00254-2.
[38] G.G. Tejani, N. Pholdee, S. Bureerat, D. Prayogo, Multiobjective adaptive symbiotic organisms search for truss optimization problems, Knowl. Based Syst. 161 (2018) 398–414.
[39] G.G. Tejani, N. Pholdee, S. Bureerat, D. Prayogo, A.H. Gandomi, Structural optimization using multi-objective modified adaptive symbiotic organisms search, Expert Syst. Appl. 125 (2019) 425–441.
[40] V. Ho-Huu, T. Vo-Duy, T. Nguyen-Thoi, L. Ho-Nhat, Optimization of truss structures with reliability-based frequency constraints under uncertainties of loadings and material properties, Appl. Math. Eng. Reliab. (2016) 59–65.
[41] A. Kaveh, A. Zolghadr, Meta-heuristic methods for optimization of truss structures with vibration frequency constraints, Acta Mech. 229 (2018) 3971–3992.
[42] A. Kaveh, S. Mahjoubi, Hypotrochoid spiral optimization approach for sizing and layout optimization of truss structures with multiple frequency constraints, Eng. Comput. **35** (2011) 1443–1462.
[43] A. Kaveh, A. Zolghadr, Cyclical parthenogenesis algorithm for layout optimization of truss structures with frequency constraints, Eng. Optim. 49 (2017) 1317–1334.
[44] A. Kaveh, A. Zolghadr, Shape and size optimization of truss structures with frequency constraints using enhanced charged system search algorithm, Asian J. Civ. Eng. **12,** (2011) 487–509.
[45] A. Kaveh, A. Dadras, A.H. Montazeran, Chaotic enhanced colliding bodies algorithms for size optimization of truss structures, Acta Mech. 229 (2018) 2883–2907.
[46] V. Ho-Huu, T. Nguyen-Thoi, T. Truong-Khac, L. Le-Anh, T. Vo-Duy, An improved differential evolution based on roulette wheel selection for shape and size optimization of truss structures with frequency constraints, Neural Comput. Appl. 29 (2018) 167–185.
[47] M. Farshchin, C.V. Camp, M. Maniat, Multi-class teaching–learning-based optimization for truss design with frequency constraints, Eng. Struct. 106 (2016) 355–369.
[48] H.M. Gomes, Truss optimization with dynamic constraints using a particle swarm algorithm, Expert Syst. Appl. 38 (2011) 957–968.
[49] Q.X. Lieu, D.T.T. Do, J. Lee, An adaptive hybrid evolutionary firefly algorithm for shape and size optimization of truss structures with frequency constraints, Comput. Struct. 195 (2018) 99–112.
[50] A. Kaveh, M. Ilchi Ghazaan, Vibrating particles system algorithm for truss optimization with multiple natural frequency constraints, Acta Mech. 228 (2017) 307–322.
[51] A. Kaveh, B. Mirzaei, A. Jafarvand, An improved magnetic charged system search for optimization of truss structures with continuous and discrete variables, Appl. Soft Comput. 28 (2015) 400–410.
[52] A. Kaveh, B.F. Azar, S. Talatahari, Ant colony optimization for design of space trusses, Int. J. Space Struct. 23 (2008) 167–181.